

## Review of Ultrawide-Bandgap (UWBG) Semiconductor Device

Author: Chaolei Zhang

Affiliation: University of Manchester

Email: chaolei.zhang@student.manchester.ac.uk



### 1. Introduction

Recently, Ultrawide-Bandgap (UWBG) semiconductor, which is defined with bandgap  $>3.4\text{eV}$  (bandgap of GaN), has been mainly researched due to its excellent performance in high power, high frequency, and high-temperature applications. The most common UWBG materials include aluminum nitride (AlN), gallium oxide ( $\text{Ga}_2\text{O}_3$ ), and diamond which have a bandgap of 6.2 eV, 4.9 eV, and 5.5 eV respectively [1].

This poster aims to take a brief review of currently existing UWBG semiconductor devices such as metal-oxide-semiconductor field effect transistors (MOSFET), metal-semiconductor field effect transistors (MESFET), and high electron mobility transistors (HEMT), analyze their performance to guide potential challenge and future developing plan.

To achieve this aim, the objectives that can be taken are listed as follows:

1. Research aluminum nitride and diamond's crystal structure and material properties.
2. Discover the structure optimization of the device in each journal paper.
3. Analyze the performance characteristics of each device.

### 2. UWBG Material Structure & Properties

AlN usually exists as an alloy with GaN, which is called  $\text{Al}_x\text{Ga}_{1-x}\text{N}$  where  $x$  is the content of aluminum in the alloy, varies between 0% to 100%. For AlGa<sub>1-x</sub>N doping, the most commonly used material is Si for n-type doping and Mg for p-type doping [1].

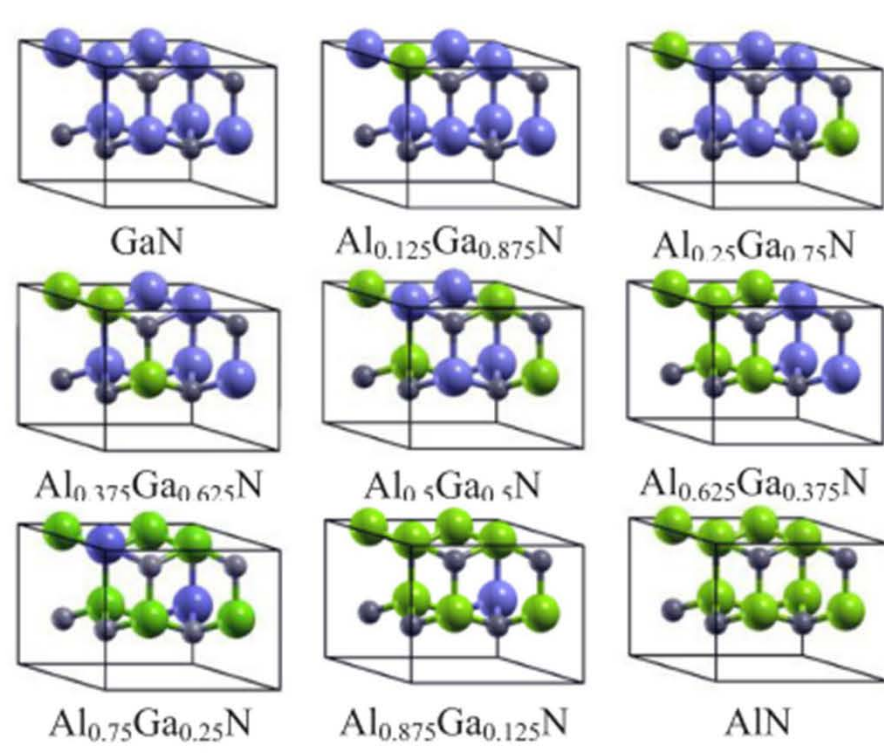


Figure 1 - Crystal Structure of AlGa<sub>1-x</sub>N [3]

Both AlN and GaN have the same crystal structure, called a Wurtzite-type structure [2] As Figure 1 illustrates, the gray ball represents N, the blue stands for Ga, and the green one is Al.

Currently, the AlN wafer in the market has a maximum size of 2 inches, with a 4-inch wafer developing in progress [4].

The diamond that is used in the UWBG application is called n-diamond, which can be seen as a metastable intermediate state between sp<sup>2</sup> graphite and sp<sup>3</sup> diamond [5].

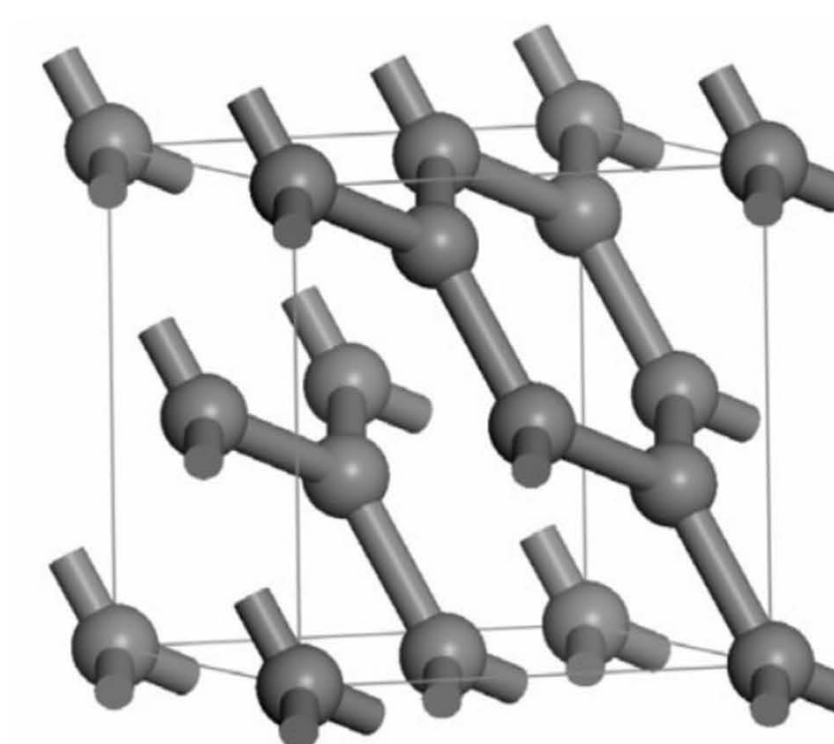


Figure 2 - Rhombohedral Representation of N-Diamond [5]

Normal sp<sup>3</sup> diamond and n-diamond have a similar structure of rhombohedral representation (Figure 2), which means 4 atoms in a unit cell with coordinates (0,0,0), (0.5,0.5,0), (x,x,x), (0.5+x,0.5+x,x), for sp<sup>3</sup> diamond,  $x$  equals to 0.25, but for n-diamond,  $x=0.355$  [5].

According to Figure 3, with a comparison among diamond,  $\text{Ga}_2\text{O}_3$ , and Al(Ga)N, Al(Ga)N has the best adaptivity, it can be used in several types of devices; while  $\text{Ga}_2\text{O}_3$  has the most limits in device application.

Properties	Diamond	$\text{Ga}_2\text{O}_3$	Al(Ga)N
Large Bandgap	Yes	Yes	Yes
Doping: n-type	Yes	Yes	Yes
Doping: p-type	Yes	Yes	Yes
High electron mobility	Yes	Yes	Yes
High hole mobility	Yes	Yes	Yes
Heterostructures	Yes	Yes	Yes
Polarization	Yes	Yes	Yes
HEMTs	Yes	Yes	Yes
IFETs	Yes	Yes	Yes
CMOS	Yes	Yes	Yes
RFET	Yes	Yes	Yes
IGBT	Yes	Yes	Yes
High thermal conductivity	Yes	Yes	Yes
Large area substrate	Yes	Yes	Yes
Semiconductor in market	Yes	Yes	Yes

Figure 3 - UWBG Material Comparison [1]

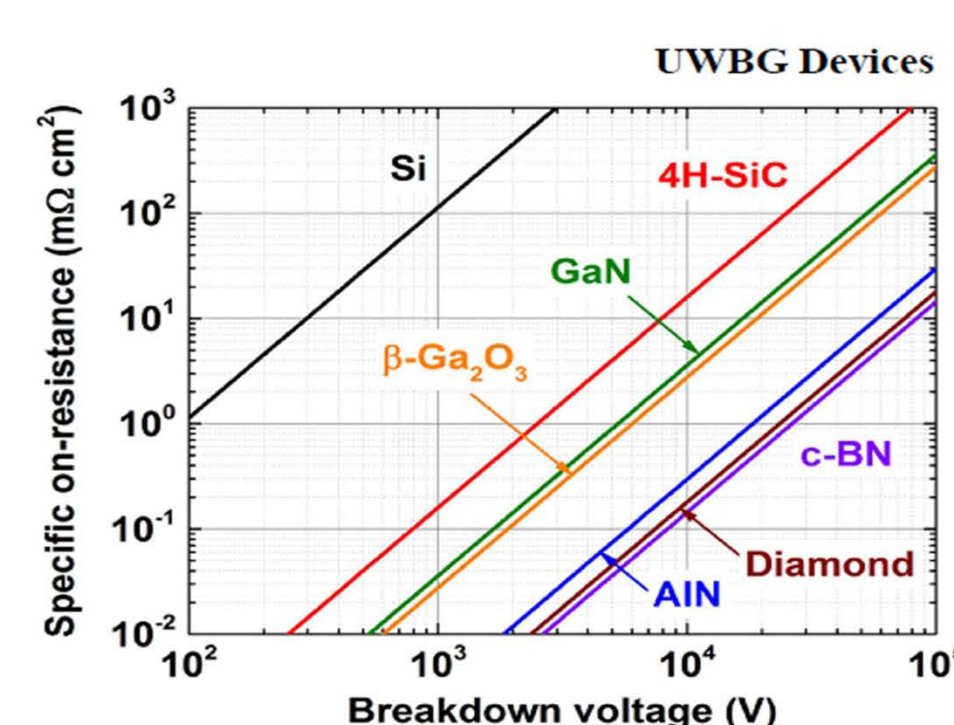


Figure 4 - UWBG Material Performance [6]

In UWBG semiconductor device research, resistance and breakdown voltage are two important parameters that need to be considered. Based on Figure 4, the closer the line of the material to the bottom right corner, the better performance it has. Hence, diamond is one of the best materials that can be used in device production.

### 3. UWBG Device Analysis & Discussion

#### 3.1 AlGa<sub>1-x</sub>N

One of the most common AlGa<sub>1-x</sub>N devices is HEMT, which mainly depends on 2-D electron gas (2DEG) existing in the channel layer to carry electron mobility. As shown in Figure 5, different from the typical gallium-polar GaN HEMT design, this AlGa<sub>1-x</sub>N HEMT takes a nitrogen-polar design to get lower contact resistance, larger drive current, and larger breakdown voltage [7].

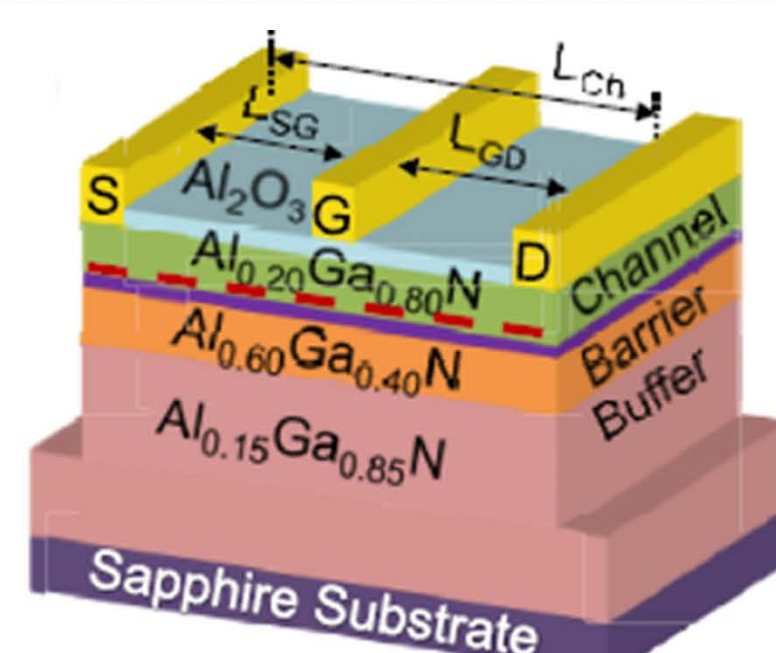


Figure 5 - N-polar AlGa<sub>1-x</sub>N HEMT [7]

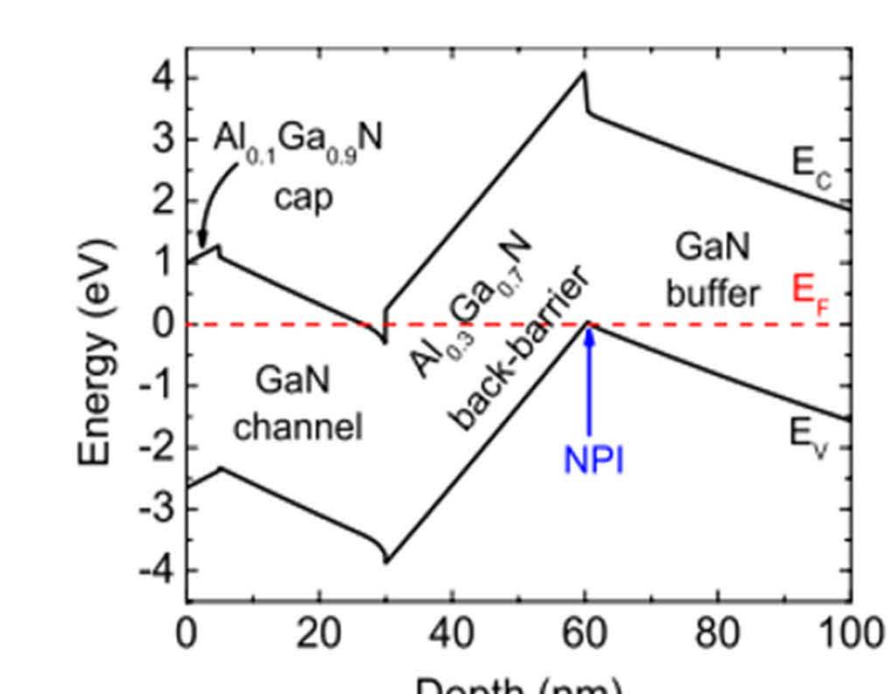


Figure 6 - Energy Band Diagram of typical non-doping N-polar HEMT [8]

Unlike typical Ga-polar structure, the 2DEG exists above the barrier layer rather than under, this is due to the opposite electric field in the N-polar structure [8]. Within this structure, 2DEG can be formed without doping, as Figure 6 illustrates, the  $E_v$  at the barrier/buffer interface without doping is only a 60meV difference from the Fermi level. Hence at this point, 2DEG can be easily formed with gate voltage bias.

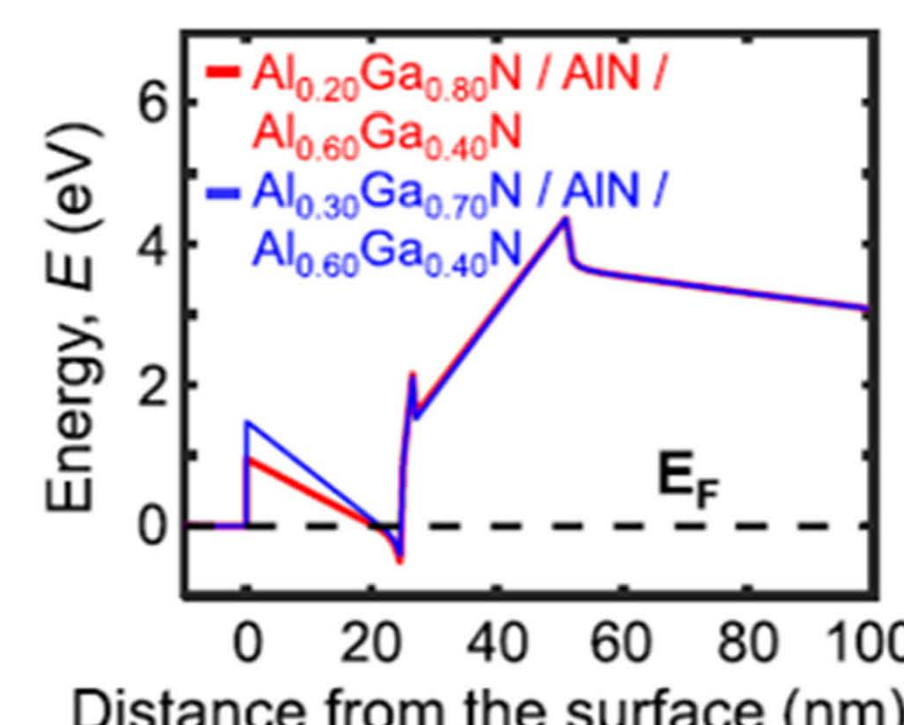


Figure 7 - Actual Energy Band Diagram of the HEMT [7]

As the energy band diagram in Figure 7 shows, in the location that the channel layer near the barrier layer (i.e. red dashed line in Figure 5), the energy is below the Fermi level, which represents the existence of 2DEG. This phenomenon supports the theory of N-polar HEMT, hence the structure is reasonable.

Also, the author provides two HEMT designs, with the same structure of 0.6 μm buffer, 25 nm barrier, 2 nm interlayer, and 25 nm channel but different Al content in a channel to investigate the effect of Al content in a channel on the device performance. The result is shown in the table below:

Channel Material	$\text{Al}_{0.2}\text{Ga}_{0.8}\text{N}$	$\text{Al}_{0.3}\text{Ga}_{0.7}\text{N}$
Drain Current (mA/mm)	250	52
Threshold Voltage (V)	-16	-20
Breakdown Voltage (V)	>400	558
Contact Resistance (Ohm*mm)	1.06	44.5

Table 1 - HEMT Performance Comparison [7]

Based on the result, the HEMT with 20% Al content in the channel layer has a better performance than the 30% Al content HEMT with a larger drain current, higher breakdown voltage, and lower contact resistance. The output characteristic and transfer characteristic diagrams of the HEMT are listed in Figures 8 and 9 respectively below:

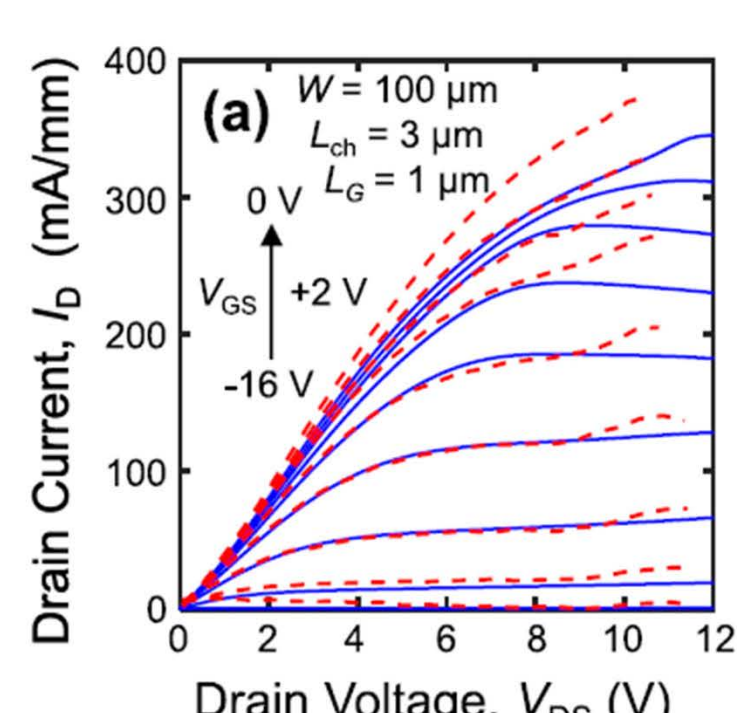


Figure 8 - HEMT Output Characteristic [7]

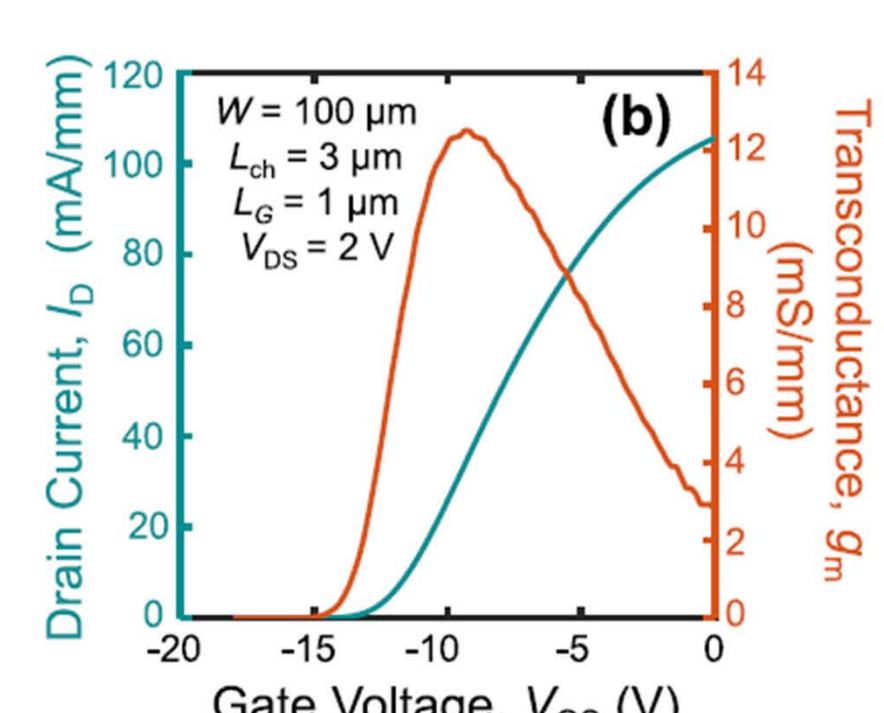


Figure 9 - HEMT Transfer Characteristic [7]

#### 3.2 Diamond

Due to material properties, diamond is most common in the application of field effect transistors, such as MOSFETs and MESFETs. Figures 10 and 11 show a MOSFET that owns an n-diamond channel with phosphorus doping, the substrate is a homoepitaxial diamond substrate.

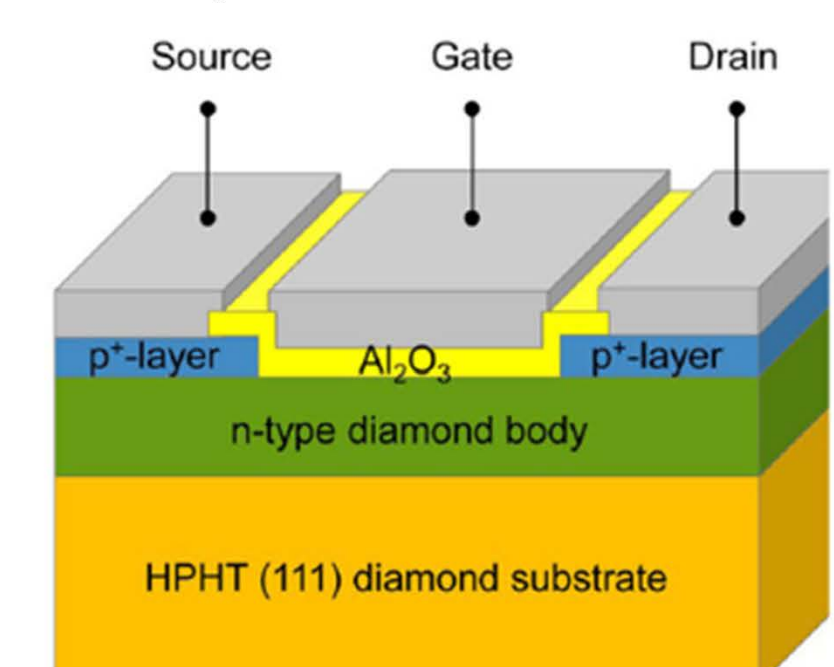


Figure 10 - MOSFET Schematic Diagram [9]

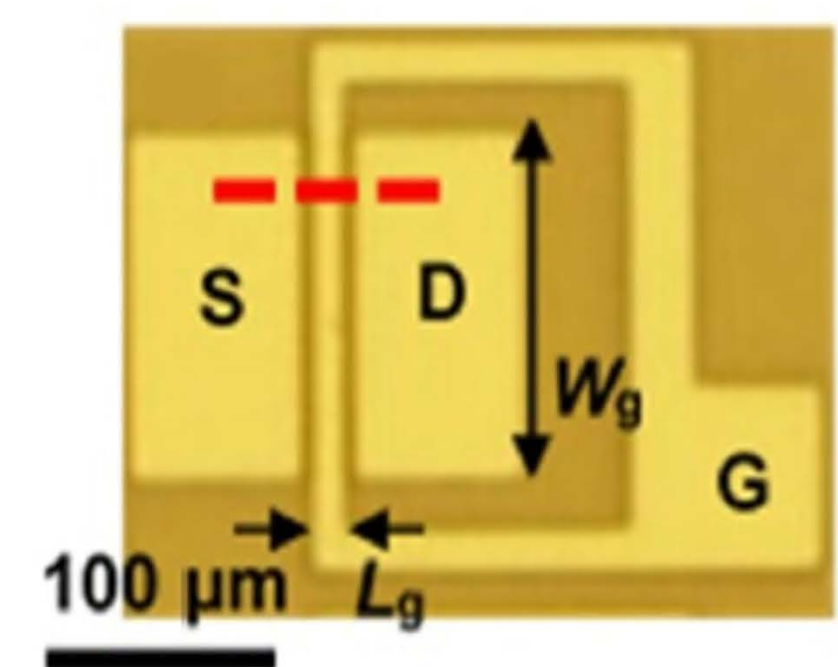


Figure 11 - MOSFET Top View [9]

The current existing n-diamond MOSFETs are hard to control their threshold voltage hence the author applies an inversion channel design (i.e. p-type channel, current flows from source to drain, negative drain current) in the n-diamond MOSFET to control threshold voltage by changing the impurity concentration in the channel [9]. According to the journal, the absolute value of threshold voltage increases as the phosphorus doping concentration increases [9]. Also, the author provides the output and transfer characteristic diagrams to illustrate the performance of the MOSFET, shown in Figures 12 and 13 below:

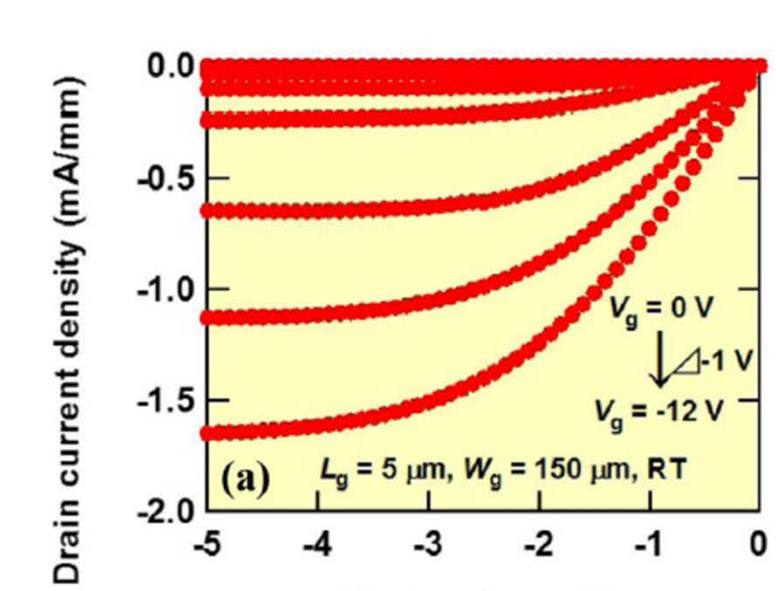


Figure 12 - Output Characteristic [9]

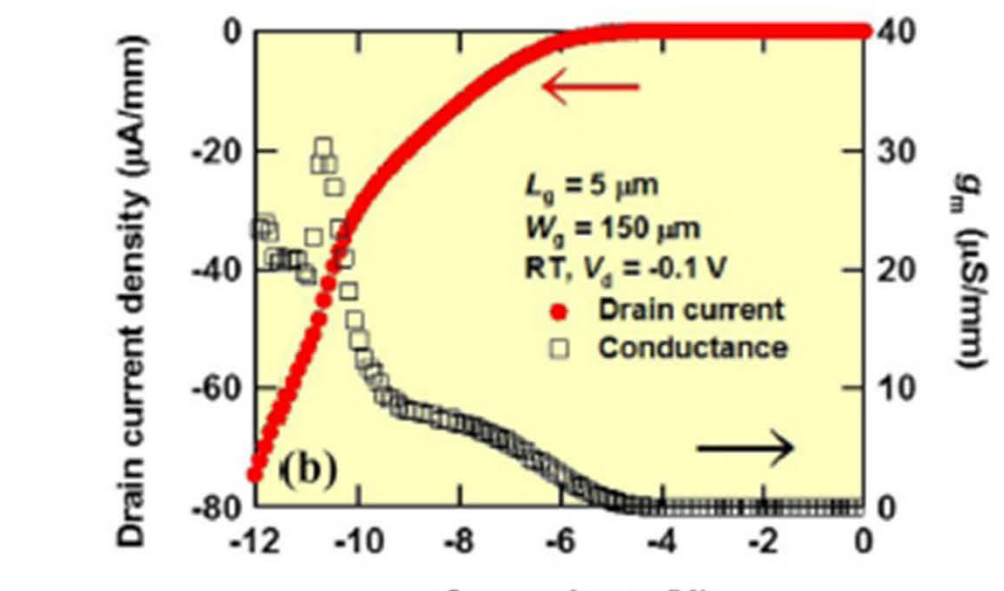


Figure 13 - Transfer Characteristic [9]

Another example of n-diamond device is MESFET, which has its schematic cross-section diagram in Figure 14. Unlike other UWBG devices, diamond devices have a terrible performance under high temperatures. As a result, this design takes heavily phosphorus-doped diamonds on the source and drain contact to optimize this circumstance [10].

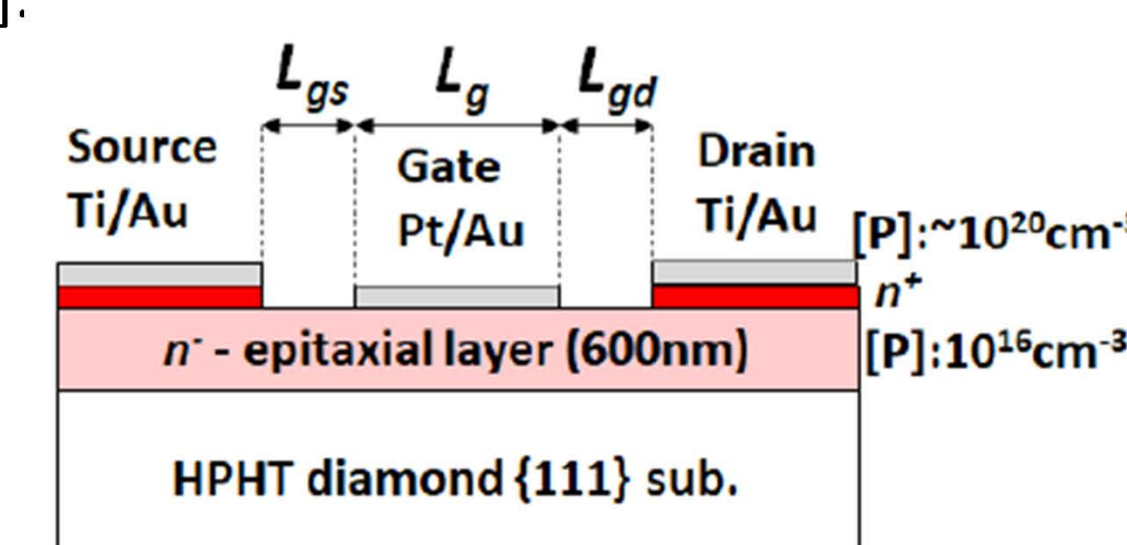


Figure 14 - MESFET Schematic Diagram [10]

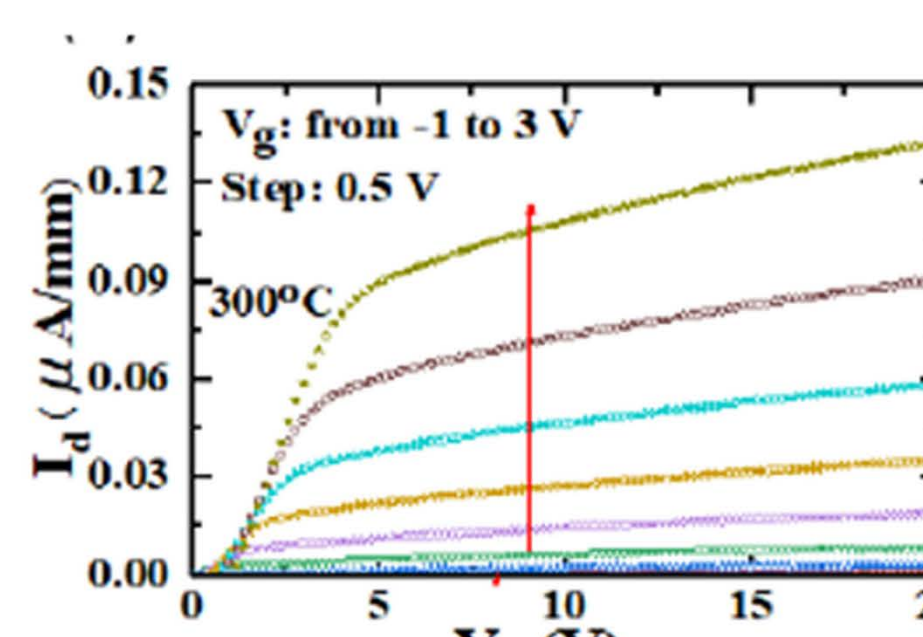


Figure 15 - Output Characteristic [10]

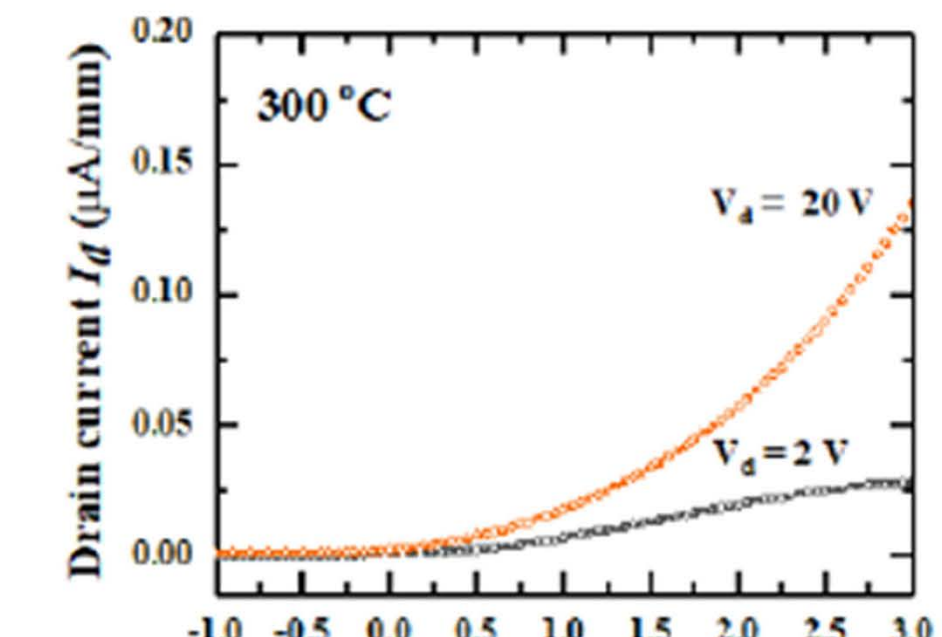


Figure 16 - Transfer Characteristic [10]

Based on the output and transfer characteristic diagrams shown in Figures 15 and 16, the optimization successfully makes the MESFET work properly in a high-temperature environment, with a threshold voltage of more than 1 V.

### 4. Conclusion

In conclusion, this poster successfully analyzes three different UWBG semiconductor devices that are made of AlGa<sub>1-x</sub>N and n-diamond, with the result diagrams of each device. Based on this poster, the audience can understand the current UWBG semiconductor device developing process, hence based on this understanding to do further research for performance optimization.

### 5. Reference

- [1] H. H. Wang, "RESEARCH ON ENGINEERING GROWTH AND TRANSFER IN HEMT GENERATION TRANSISTORS ON AIN PLATFORM," Ph.D. dissertation, Cornell Univ., Ithaca, 2022. Available: <https://search.proquest.com/docview/2514744444?pq-origsite=scholarlink>
- [2] E. H. H. Wang, and P. A. Brown, "Structure and properties of AlN," Physical Review B, vol. 46, no. 11, pp. 7157-7173, Mar. 1992. doi: <https://doi.org/10.1103/PhysRevB.46.7157>
- [3] J. L. Li, T. Li, C. Li, and S. Zhu, "Composition dependence of phonon and thermodynamic properties of the ternary AlGa<sub>1-x</sub>N mixed crystal," British Journal of Applied Physics, vol. 14, pp. 1025-1026, Sep. 1973. doi: <https://doi.org/10.1088/0022-3778/14/9/005>
- [4] G. L. Cao, "Recent Advances in Nitride Technology," Crystal Growth, vol. 19, no. 1, pp. 1-10, 2018. Available: <https://www.scienceopen.com/document?doi=10.1515/cryst.2018.001> (accessed Jul. 25, 2024).
- [5] R. Wang, J. Zhou, and E. L. Yu, "Synthesis and crystal structure of n-diamond," International Materials Review, vol. 52, no. 3, pp. 131-151, May 2007. doi: <https://doi.org/10.1179/17442000701402218>
- [6] A. J. S. Jones, A. B. S. Jones, M. S. Grimes, and M. A. Green, "Theoretical Challenges in the UWBG Semiconductors AlGa<sub>1-x</sub>N, Diamond, and Ga<sub>2</sub>O<sub>3</sub> Must Move to Conquer with SiC and GaN HET Devices," ECS Transactions, vol. 40, no. 7, 2023. doi: <https://doi.org/10.1149/2023-02.0000000000000000>
- [7] W. N. H. H. Wang, and S. Choudhary, "Demonstration of N-Polar AlGa<sub>1-x</sub>N High Electron Mobility Transistors With 375 mA/mm Drain Current," IEEE Electron Device Letters, vol. 44, no. 7, pp. 1072-1075, Jul. 2023. doi: <https://doi.org/10.1109/EDL.2023.3272955>
- [8] W. N. H. H. Wang, "The gate voltage and high electron mobility transistors," Semiconductor Science and Technology, vol. 28, no. 7, p. 074009, Jun. 2013. doi: <https://doi.org/10.1088/0268-1221/28/7/074009>
- [9] X. Zhang, T. Kozumoto, S. Yamazaki, C. E. Nebel, T. Nakamura, and N. Tokuda, "Inversion-type p-channel diamond MOSFET device," Journal of Materials Research: Process & Applications, vol. 36, no. 23, pp. 4688-4702, Aug. 2023. doi: <https://doi.org/10.1002/jmr2.1212>
- [10] Takahiro Shimada, M. Liu, and S. Kozuma, "76-Type Diamond Metal-Semiconductor Field-Effect Transistor With High Operation Temperature of 300°C," IEEE Electron Device Letters, vol. 41, no. 4, pp. 588-591, Apr. 2020. doi: <https://doi.org/10.1109/EDL.2020.2931515>

